



# Mechanical and metallurgical characterization of AA6082-T6 sheet-bulk joints produced through a linear friction welding based approach

Gianluca Buffa<sup>1</sup> · Dario Baffari<sup>1</sup> · Antonio Barcellona<sup>1</sup> · Davide Campanella<sup>1</sup> · Livan Fratini<sup>1</sup>

Received: 13 May 2019 / Accepted: 9 October 2019 / Published online: 3 January 2020  
© Springer-Verlag France SAS, part of Springer Nature 2020

## Abstract

In the last decades, new flexible manufacturing processes have been developed to face the demands, by many industrial fields, for highly customized complex functional parts. The peculiar design of these components often overcomes conventional sheet metal and bulk metal forming processes capabilities. In order to face this issue, new hybrid techniques, capable of exploit key advantages of different processes, have to be developed. In this study, a method to obtain sheet-bulk joints, based on the Linear Friction Welding process, is proposed. The feasibility of the technique was investigated through an experimental campaign carried out with varying pressure and oscillation frequency using AA6082-T6 aluminum alloy. The main mechanical and metallurgical properties of the produced joints, including typical material flow defects, were highlighted. It was found that sound hybrid sheet-bulk joints can be produced by the proposed approach. Finally, it was highlighted how the height of the weld center zone plays a key role on the mechanical properties of the produced joints.

**Keywords** Linear friction welding · Sheet-bulk · Aluminum alloys · Microstructure

## Introduction

The development of manufacturing technologies and the research for performant solutions is leading to the wide use of light materials in most industrial application. These materials (i.e. aluminium, magnesium and titanium alloys) are characterized by a high strength/weight ratio, allowing the production of light structures without using expensive composite

materials. However, advanced welding technologies are needed to produce these structures made of “difficult to weld” or “non-weldable” metals and characterized by complex geometries. The peculiar design of these components often overcomes conventional processes capabilities, requiring new manufacturing routes and technologies to be developed. In order to face these issues, hybrid techniques capable of exploit key advantages of different processes have been proposed in the last decades [1]. In particular, hybrid structures, characterized by both sheet and bulk components, have been investigated by a few researchers as an exemplary symbiosis between additive and subtractive technologies [2] or complex sheet-bulk forming operation [3, 4]. Schaub et al. [5] used LBM technology to additively manufacture functional elements on titanium alloy sheet for biomedical applications. They investigated the influence of the process parameter on the additively manufactured pin shear strength, while Papke et al. [6] dealt with the bending of such components. A more in-deep analysis of the mechanical properties of these hybrid components has been carried out by Schaub et al. [7]. The production of these structures could be simplified by using effective sheet-bulk joining techniques that could substitute and/or integrate the above-cited hybrid manufacturing routes.

---

✉ Gianluca Buffa  
gianluca.buffa@unipa.it

Dario Baffari  
dario.baffari@unipa.it

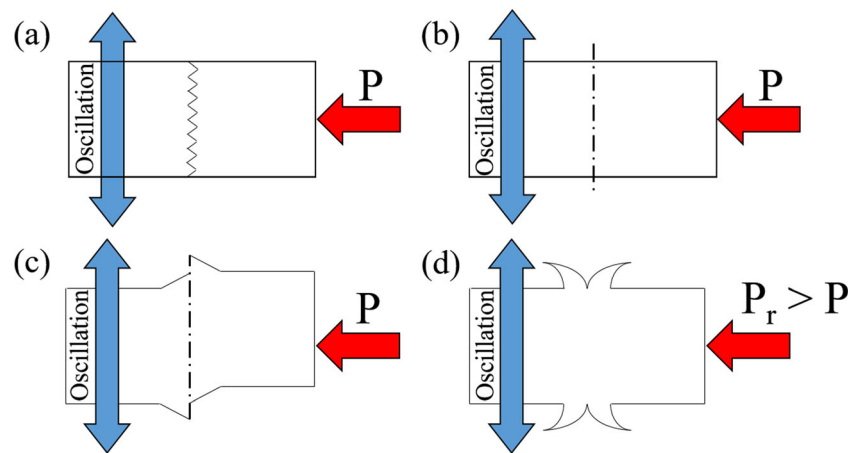
Antonio Barcellona  
antonio.barcellona@unipa.it

Davide Campanella  
davide.campanella@unipa.it

Livan Fratini  
livan.fratini@unipa.it

<sup>1</sup> Department of Engineering, University of Palermo, Viale delle Scienze, 90128 Palermo, Italy

**Fig. 1** The four LFW stages: (a) initial, (b) transition, (c) equilibrium and (d) deceleration stage



Linear Friction Welding is a candidate to face this challenge since its unique process mechanics allows for effective welding in the whole joint area.

Linear Friction Welding (LFW) is a solid-state joining process designed to weld bulk non axis-symmetrical components and it can be applied both to dissimilar or homologous joints. During the process, the two parts to be welded are put in contact by a given force while a reciprocating motion is onset in order to generate friction at the separation interface. The whole process can be divided into four fundamental distinct phases [8, 9] (Fig. 1): first, the workpieces are brought into contact (the initial contact surface is actually less than the area of welding because of the micro-roughness). Hence, the oscillatory motion and the closing pressure cause the surface roughness to be quickly reduced increasing the contact area and the heat generation through friction. If the generated heat flux is adequate, the process moves to the “transition” stage in which the increase of temperature causes the softening of the metal at the interface. The softening obtained causes the sideward extrusion of the material that produces the typical “flash”, reducing the height of the workpieces (burn-off) during this “equilibrium” phase. Finally, the motion of the adjoining pieces is quickly arrested and the closing pressure is increased in order to complete the welding process. The main process parameters affecting LFW are interface pressure,

oscillation frequency, oscillation amplitude (commonly sinusoidal) and duration of the process. It should be observed that total burn-off could be used as a process parameter instead of time. However, in LFW process, it is usually preferred time because of the difficulties in accurate control as high burn-off rate occurs during the equilibrium phase.

All the stages and their evolution are influenced by the process parameters that are deeply linked to each other causing the process itself to be difficultly engineerable, as it requires a dedicated experimental campaign to fine-tune the process for every used material. For example, an increased frequency of the oscillation could certainly require a smaller amplitude of the movement to keep proper welding conditions.

LFW is one of the oldest friction based welding processes but has been quickly developed only in the last years and relatively few papers can be found in literature regarding machine construction [10] and welding of titanium alloys [11], aluminum alloys [12], steels [13], nickel-based alloys [14], and dissimilar joints [15–18]. This lack of knowledge is due to a few reasons. On the one hand, LFW machines cannot be obtained adapting common machines (as happens for other friction welding technologies i.e. FSW and RFW) and dedicated commercial machines are often too expensive and unsuited to research studies. On the other hand, the technology

**Fig. 2** Sketch of the machine

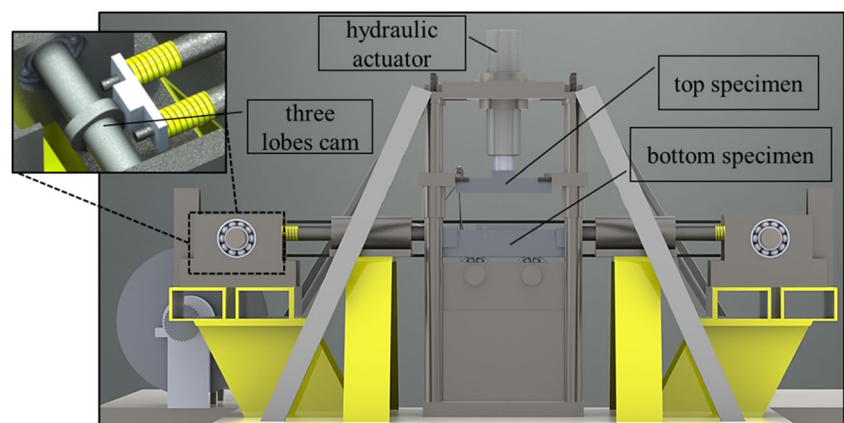


**Table 1** Chemical composition of the used alloy

Material %	Mn	Fe	Mg	Si	Cu	Zn	Ti	Cr	Others
<b>AA6082</b>	0.41.0	0.0	0.6	0.7	0.0	0.00.2	0.0	0.0	0.0
		0.5	1.2	1.3	0.1		0.1	0.25	0.05

results to be complex due to the above mentioned mutual interaction of process parameters.

In this paper, the feasibility of a LFW based approach to produce hybrid sheet-bulk joints is investigated. An experimental campaign was carried out using AA6082-T6 aluminium alloy to give an insight into the effects of the main process parameters on the solid bonding effectiveness, evaluated through the analysis of the main mechanical and metallurgical properties of the joints. A few differences with respect to conventional LFW are highlighted. Finally, a metallurgical parameter was identified as the main link between the process parameters and the joints mechanical performances.

## Proposed approach

### The developed machine

The experimental campaign was carried out on an in-house designed and built experimental machine [19]. This machine uses a desmodromic kinematic chain to create the needed reciprocating motion of the bottom specimen. Two cams with three lobes profile are placed on two parallel shafts connected by coupling belt and pulleys. A hydraulic actuator was fixed on a steel rank and controlled by an electro-valve, allowing loads up to 15 kN. A virtual instrument controls the hydraulic electro-valve and a switch is used as a trigger to determine the beginning and the end of the test trial. The virtual instrument

sets the pressure on the actuator in an assigned period and controls all the other devices and sensors connected to the machine (e.g. clutch, torque meter and accelerometer). The pneumatic clutch, positioned on a secondary shaft connected to the machine by coupling chain and reels, allows a quick stop of the oscillation reducing the machine inertia [12]. Figure 2 presents a sketch of the experimental machine.

### Materials and methods

The specimens were obtained from AA6082-T6 aluminium alloy sheets, 2 mm in thickness, and bars. The base material was characterized, at room temperature, by yield stress of 276 MPa and ultimate tensile stress (UTS) of 323 MPa. Table 1 sums up the chemical composition of the investigated alloy, while in Fig. 3a a sketch of the bulk and sheet samples used for the welding experiments is presented. The surface to be joined did not undergo any particular preparation before the welding process took place.

The experimental campaign was carried out with varying oscillation frequency and applied pressure, while oscillation amplitude and process time were kept constant. Oscillation was given to the sheet while pressure was applied on the bulk part. Two holes were drilled on the sheet which was bolted on the oscillating backing plate of the machine in order to have a perfect fix. The investigated process parameters are summarized in Table 2. The process parameters were selected according to previous experimental campaigns of conventional LFW on similar alloys [20]. It is worth noting that all the process parameters have an influence on the heat input into the joint. However, the results presented in [17] show that a quite wide range of different weld conditions, i.e. insufficient heat, sound joints and instability (excess of heat), can be reached by properly varying just pressure and oscillation frequency. For this reason, in this initial study on the sheet-bulk LFW welding of

**Fig. 3** (a) Sketch of the welding samples (dimensions in millimetres) and (b) reference axes

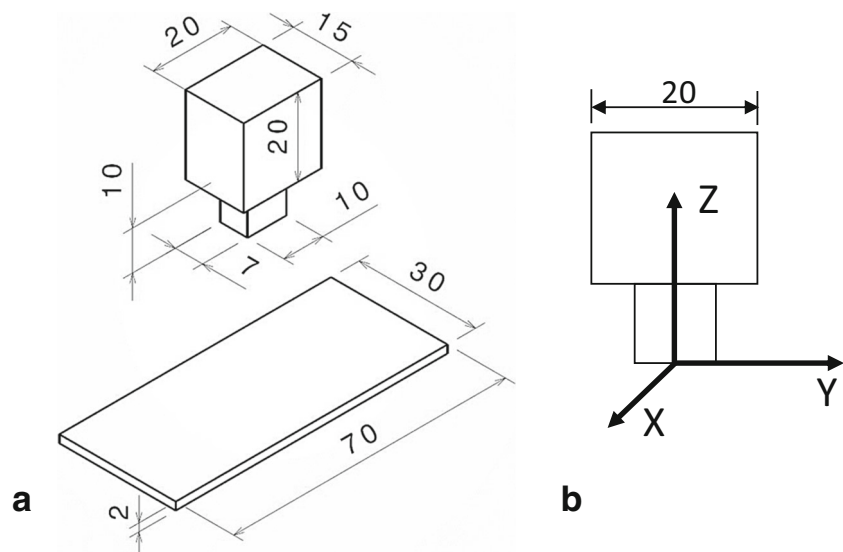


**Table 2** Process parameters ranges

Process parameters		Value(s)
Frequency	$f$ [Hz]	45, 56, 72
Pressure	$p$ [MPa]	21, 32, 42
Amplitude	$a$ [mm]	3
Time	$t$ [s]	3.87

aluminum alloys, a “2D” experimental plan, obtained keeping constant process time and oscillation amplitude, was utilized. Each test was repeated three times to assess repeatability. The welds were saw cut, mounted, and polished to carry out microhardness measurements along the joint cross section orthogonal to the X axis. In particular, the measurement points were taken along the Z axis shown in Fig. 3b with a pitch of 0.5 mm. Metallurgical observations have been carried out after 30s chemical etching with a 0.5% vol. water solution of hydrofluoric acid. Three-point bending of the joint (punch on the opposite side with respect to the welded bulk part) and tensile tests (along the direction orthogonal to the welding surface) were performed in order to investigate the joints’ mechanical properties. For these tests the flash was mechanically removed. It is worth noticing that, given the peculiar joint geometry, the tensile tests have the aim to compare the investigate case studies.

## Results and discussion

### Heat input and morphological characterization

One of the main factors influencing the LFW process is the heat input induced by the friction forces. In order to globally take into account the contribution of the different process parameters on the heat generation, the  $W$  parameter was calculated for all case studies [21]. In particular, the parameter is

calculated using the root mean square of amplitude, angular frequency and pressure at the interface [12]:

$$W = \frac{2\pi f a p}{\sqrt{2}} \text{ [kW/mm}^2\text{]} \quad (1)$$

Table 3 summarizes the investigated case studies, while Fig. 4 shows the utilized process window with varying  $W$ , as a function of the oscillation frequency (Eq. 1).

It is worth noticing that the ID1 case study (highlighted in red in Fig. 4) did not produce an effective weld since the joint failure occurred during the sample cutting operation. This incipient bonding phenomenon is typical of LFW processes characterized by too low heat input which results into the welding of only a very small area in the centre of the adjoining surfaces, as it was observed in previous studies on LFW [22]. Figure 5 shows the three joints obtained using the intermediate value of pressure and varying frequencies, resulting in different  $W$  values. It is worth noticing that higher heat input is required, with respect to conventional LFW [20], for the considered process conditions due to the need to compensate for the elevate heat loss in the weld zone caused by the conductivity and heat exchange with environment of the sheet. Additionally, less flash is observed with respect to “conventional” LFW because the sheet behaves as a “infinite plane” not participating to the flash formation. From the figure, it is observed that ID2 does not show sufficient flash formation. In this case, poor mechanical properties can be expected. Flash formation increases with heat input, reaching a qualitatively acceptable level for ID5 and ID8.

### Mechanical characterization

The mechanical properties of the produced sheet-bulk joints have been first assessed by tensile tests. Figure 6 shows the results obtained for the considered case studies.

Poor mechanical strength is found for the two welds produced with the lowest value of oscillation frequency. As the

**Table 3** Case Studies

ID #	Pressure P [Mpa]	Frequency f [Hz]	Amplitude a [mm]	Time t [s]	Specific heat W [kW/mm <sup>2</sup> ]
1	21	45	3	3.87	13
2	32	45	3	3.87	19
3	42	45	3	3.87	25
4	21	56	3	3.87	16
5	32	56	3	3.87	24
6	42	56	3	3.87	31
7	21	72	3	3.87	20
8	32	72	3	3.87	31
9	42	72	3	3.87	40

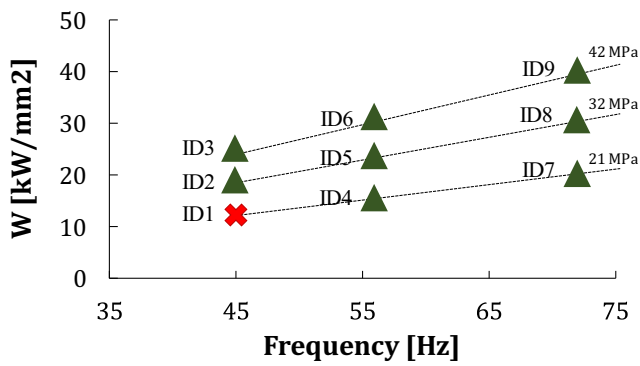


Fig. 4 The process window for the nine investigated cases studies

oscillation frequency increases, larger values of UTS can be observed with a maximum of 251 MPa, corresponding to a joint efficiency, i.e. the ratio between the UTS of the joint and the one of the parent material, of about 78%. Additionally, two different trends can be observed: a decreasing one, obtained with fixed oscillation frequency and varying pressure, i.e. with increasing specific heat *W*; a trend showing a maximum, obtained with fixed pressure and varying frequency. It is worth noticing that the first trend does not hold true for the lowest value of oscillation frequency. The reasons for this behavior will be investigated in the next paragraph. SEM analyses of the fracture surfaces were undertaken on the broken specimens. In Fig. 7 the images of the fractured surfaces of the ID2, ID5 and ID8 case studies are reported. These case studies are characterized by the same pressure value and varying

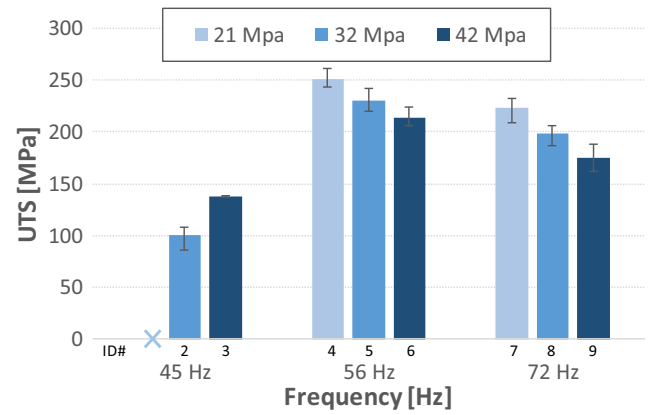


Fig. 6 Tensile test results for the considered case studies

oscillation frequency, resulting in increasing specific heat. It was noted that, for the considered case studies, fracture occurred on a plane parallel to the oscillation plane below the original separation surface between the parts. Additionally, fracture surface appeared quite homogeneous all over the bulk element bottom surface.

From the figure it can be observed that the ID8 sample (see Fig. 7a) shows an intergranular fracture due to the decohesion of the crystalline grains at the grain edge. On the other hand, the ID2 sample is characterized by transgranular fracture, as circular dimple like structures can be found in the central area. Finally, for the ID5 case study, a combination of both the failure modes occurs, with areas characterized by a more intergranular fracture (right side of Fig. 7b) and areas with a transgranular surface fracture (left side of Fig. 7b). In this way it can be stated that as specific heat decreases, fracture changes from intergranular to transgranular with a more brittle behavior.

The results of the bending tests, in terms of maximum stroke at fracture, are shown in Fig. 8. As observed for the tensile tests, ID2 case study is the one showing the lowest value. Two trends can be identified also for this test: in fact, maximum punch displacement before fracture increases both with fixed pressure and varying frequency, and with fixed frequency and varying pressure. In other words, joint ductility increases with increasing specific heat.

Finally, microhardness measurements have been carried out. The profiles obtained for ID2, ID5, ID8, ID4 and ID6 are shown in Fig. 9.

A few interesting observations can be made. First, a softened zone can be identified along the Z axis in the cross section. For the welds characterized by higher specific heat, i.e. ID8 and ID6, the weld area, namely the area in which reduced hardness with respect to parent material is observed, begins at about half thickness of the sheet (see vertical dotted lines in Fig. 9). For colder welds, i.e. ID2 and ID4, the softening effect of the welding process on the sheet material involve a thickness of 0.5 mm.

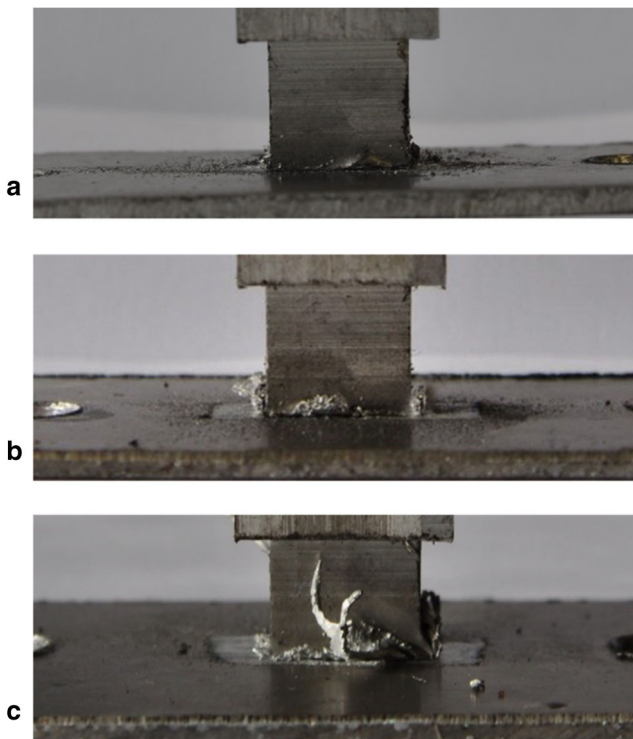


Fig. 5 Flash formation of the (a) ID2–45 Hz and 19 kW/mm<sup>2</sup>, (b) ID5–56 Hz and 24 kW/mm<sup>2</sup> and (c) ID8–72 Hz and 31 kW/mm<sup>2</sup>



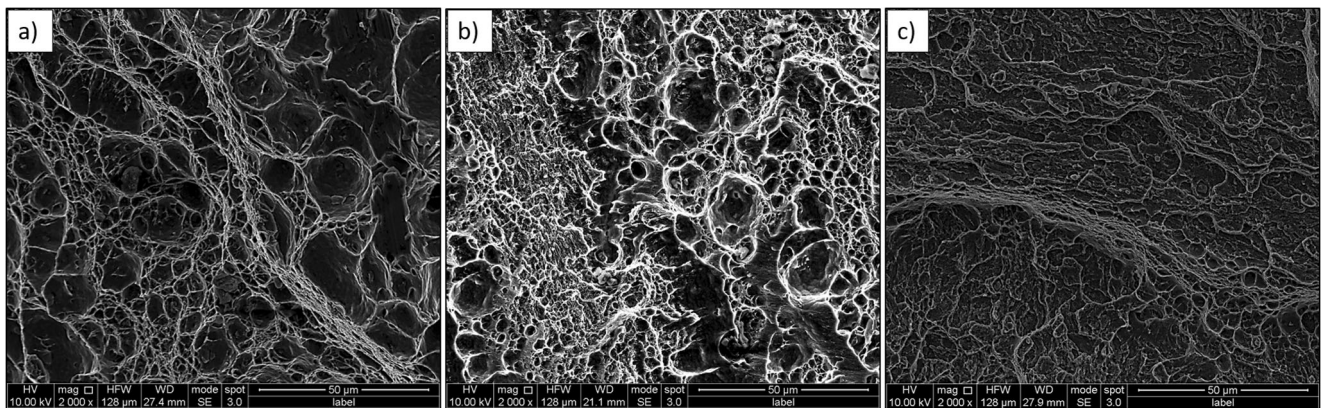


Fig. 7 SEM images of the fracture surface for (a) ID8, (b) ID5 and (a) ID2

As far as the bulk part is considered, reduced hardness is measured till a distance from the welding line of about 5.5 mm, being this value quite constant for all the considered case studies. Second, a minimum is observed in the hardness profile: this is particularly noticeable for hotter welds, for which microhardness drops, in correspondence of the weld line, to about 70 HV; on the contrary, almost no minimum is observed for the coldest welds. It can be noted that these trends are consistent with the results of the tensile tests, for which higher mechanical strength was found for colder welds, with the exception of ID2. The reasons for this behavior will be analyzed in the next paragraph. Overall, it can be stated that average HV increases with decreasing specific heat, both considering fixed pressure with increasing frequency (ID2, ID5 and ID8) and fixed frequency with increasing pressure (ID4, ID5, ID6). It is worth noticing that ID6 and ID8 are characterized by the same specific heat, although obtained with a different combination of process parameters. The resulting mechanical properties are similar but not equal. In order to further investigate on this point, the results of the metallurgical analyses have to be considered.

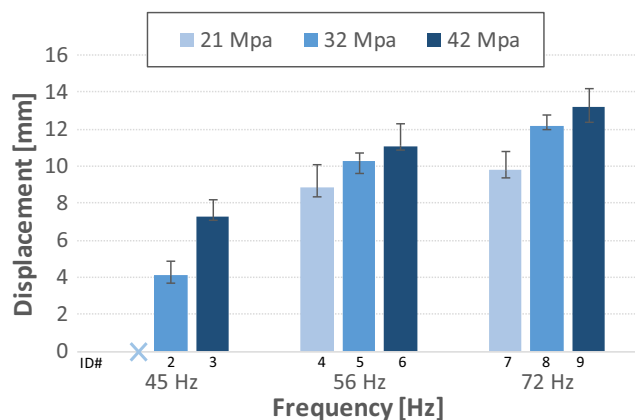


Fig. 8 Bending test results for the considered case studies

## Metallurgical characterization

In order to investigate the reasons for the mechanical properties observed and to analyze the influence of the process parameters on the solid bonding effectiveness, the specimens were characterized under the metallurgical point of view. Fig. 10 shows the typical microstructure characterizing the cross section of a sound sheet-bulk linear friction welded joint (ID8). The bulk parent material (Fig. 10b) is characterized by elongated grains, deformed along the extrusion direction. Coming closer to the original separation surface between the two specimens, a thermo-mechanically affected zone (TMAZ) is found. In this area the grains grow because of the heat input, and are heavily deformed along the oscillation direction near the boundary with the weld center. Figure 9c shows the fine equiaxed microstructure characterizing the weld center zone (WCZ). This texture results from dynamic recrystallization phenomena occurring in this highly deformed area and it is typical of most solid-state welding processes [17, 19]. It is worth noticing that this area extends below the original separation line between the specimen, i.e. involves the sheet material, consistently with what observed during the microhardness measurements. Finally, the sheet parent material, with

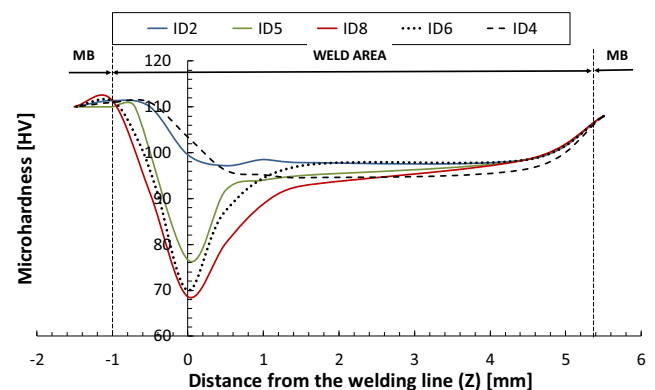
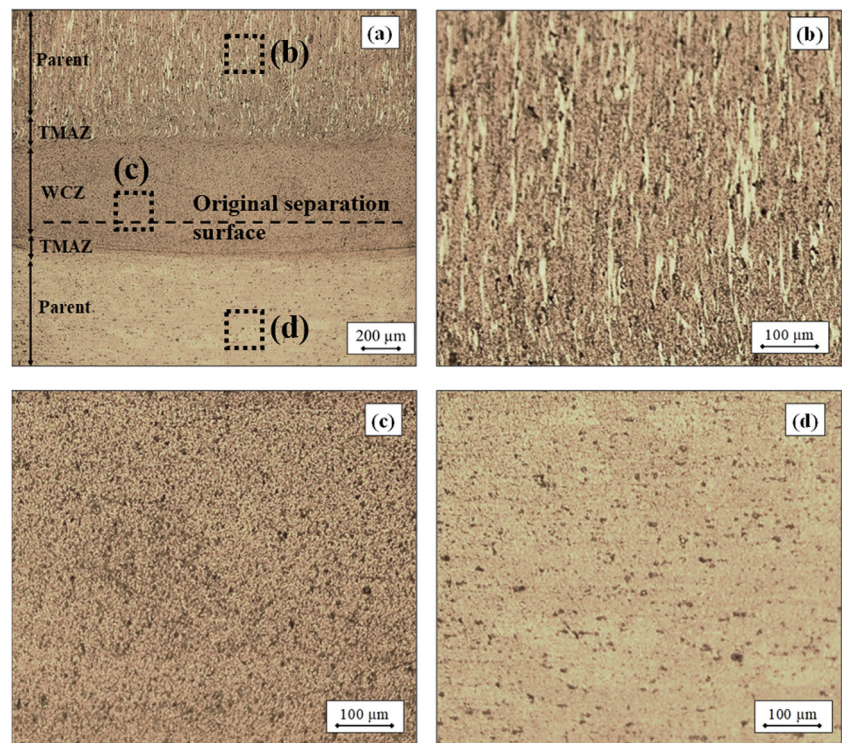


Fig. 9 Microhardness profiles for selected case studies

**Fig. 10** (a) micrograph of the cross section of the ID8 case study, with details of (b) bulk parent material, (c) Welded Zone and (d) sheet parent material



grain deformed along the rolling direction (parallel to the oscillation movement), is shown in Fig. 10d.

The range of process parameters taken into account allowed to highlight a few material flow defects having a detrimental effect on the load bearing capabilities of the joints. In particular, a combination of process parameters producing low specific heat can result in two different defects. First, a flash zone defect can occur. Fig. 11 shows the flash zone for ID2 and ID 8 case studies.

From the figure it arises that considering the ID2 case study, the WCZ was not formed in the side of the specimens. Being the specific heat too low, insufficient material softening was reached and a large void area was formed between the bottom surface of the bulk specimen and the top surface of the sheet. This kind of defect, besides reducing the resistant

section of the joint, creates a weak point in the joint for the crack propagation during a tensile test. In this way, the failure loads of the joints are significantly lower than the ones in which this condition does not occur (ID8, see Fig. 11b).

The second defect type occurs in the WCZ. Figure 12 shows the weld center for ID2 and ID8, respectively.

Again, low heat input caused ineffective solid bonding. Due to the poor material softening, three main phenomena occur: vortex-like areas can be identified, in which the material is heavily deformed but cannot bond due to the low temperature; as a consequence, voids and cracks are formed, extremely reducing the mechanical properties of these joints. Finally, it is worth noting that, although oxides analysis was not carried out in this study, it is likely that high presence of oxides, further inhibiting correct material flow, can be found

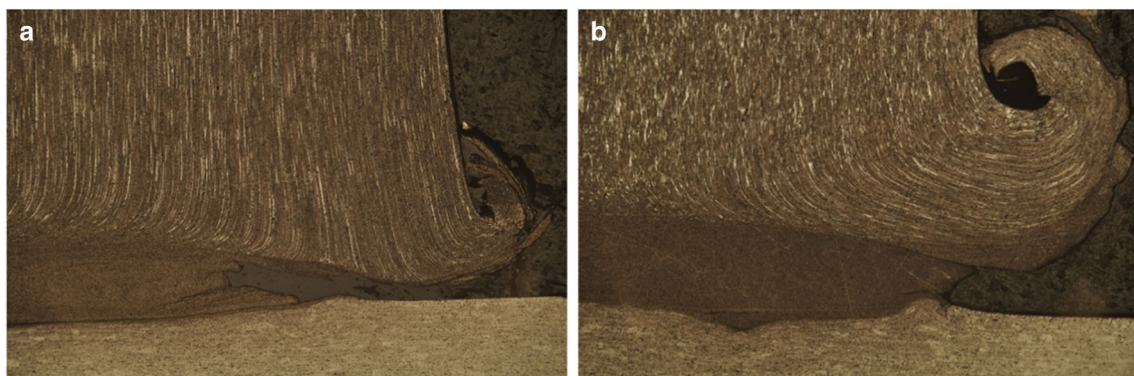
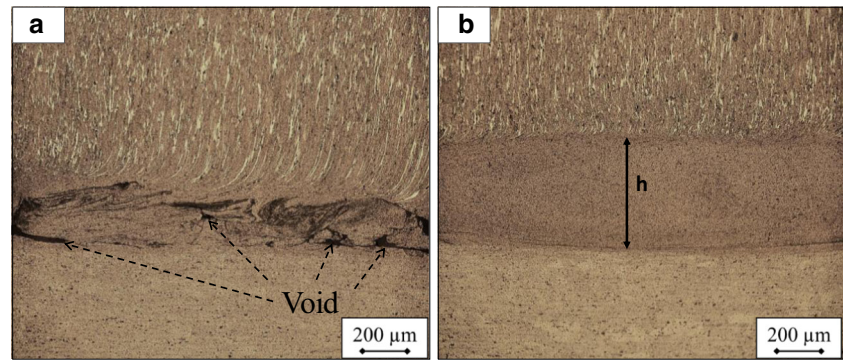


**Fig. 11** flash zone for the (a) ID2 and (b) ID 8 case studies



**Fig. 12** WCZ for the (a) ID2 and (b) ID 8 case studies



in this area. In fact, in linear friction welding processes, matching surfaces are not cleaned before welding. In LFW, the process mechanics allows the expulsion of surface oxides through flash during the equilibrium stage of the process. When this stage is too short and poor flash is formed, surface oxides remains entrapped in the WCZ, resulting in flow defects and/or embrittlement of the joint [23]. The above observations can explain the poor results obtained during both tensile and bending tests for ID2 and ID3 in spite of the relatively high hardness in the WCZ with respect to other case studies.

Finally, the average height  $h$  of the WCZ area (see Fig. 12) was measured in order to put in relation the effect of process parameters on joint metallurgical properties with mechanical properties. Figure 13 shows the average value of  $h$  and the utilized specific heat  $W$  for ID5, ID6, ID8 and ID9.

Overall, the height of the WCZ increases with increasing specific heat. However, it is worth noticing that ID6 and ID8 are characterized by the same heat input, although obtained with a different combination of oscillation and pressure. In particular, larger value of  $h$  is measured for the ID8 case study, i.e. the one characterized by larger oscillation frequency. Being the process time fixed, it can be argued that the higher number of cycles results in an enhanced involvement of material in the “high strain-high temperature” zone characterizing the WCZ. As the correspondent mechanical properties are

considered, although characterized by similar minimum hardness, ID6 HV profile shows a smaller area interested by low hardness, resulting in better mechanical strength and worse ductility. Hence, from the combined observation of the obtained results, for defect-free joints, it can be observed that the height of the WCZ has a strict correlation with the joints’ mechanical performances: an increase of  $h$ , i.e. an increase of the extension of the area where recrystallized grains are found, results in increased ductility as smaller grains acts as “buffer” to withstand bending. On the other hand, reduced strength is obtained as lower hardness can be measured over a larger area. It is worth pointing out that in friction welding processes (FSW, LFW, etc.), for precipitation hardening alloys, as the one considered in this study, the recrystallized area is characterized by reduced HV values due to the loss of the effect of the parent material thermal treatment caused by the heat generated during the process.

## Conclusions

In this paper, the feasibility of a LFW based approach to produce AA6082-T6 aluminium alloy sheet-bulk joints was investigated through an experimental campaign. From the obtained results the following main conclusions can be drawn:

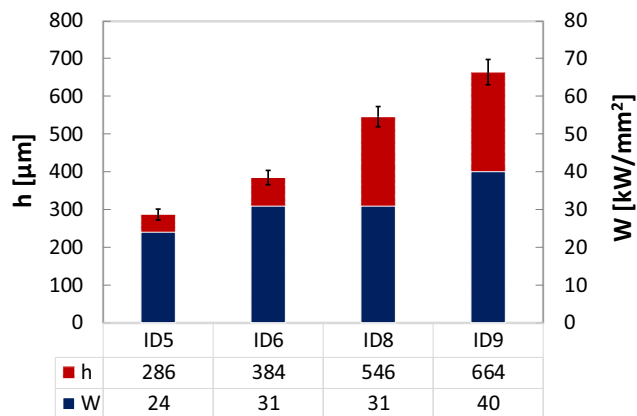


**Fig. 13** Average height of the WCZ  $h$  and specific heat  $W$  for ID5, ID6, ID8 and ID9 case studies

- Defect free sheet-bulk joints can be produced by properly selecting process parameters;
- The peculiar joint geometry causes a few variations in the process mechanics with respect to conventional LFW process: the relevant heat dispersion caused by the joint geometry requires higher heat generation with respect to conventional LFW while lower flash formation is observed;
- Too low heat input results in the presence of two different defects: a side defect in the flash area and a weld center defect. The latter is characterized by voids, vortexes and not expelled oxides because of the reduced flash formation;
- The height of the weld center can be identified as a key indicator of the mechanical properties of the joints: larger



values result in enhanced ductility and lower strength. This parameter is mainly influenced by the specific heat; however, when the same specific heat is conferred to the joint, larger oscillation frequency results in larger h values.

Future developments include an in-depth analysis of the WCZ and the set up of a dedicated numerical model able to predict its extension and metallurgical properties as a function of the main process parameters.

### Compliance with ethical standards

**Conflict of interest** The authors declare that they have no conflict of interest.

### References

- Lauwers B, Klocke F, Klink A et al (2014) Hybrid processes in manufacturing. *CIRP Ann - Manuf Technol*. <https://doi.org/10.1016/j.cirp.2014.05.003>
- Ahuja B, Schaub A, Karg M et al (2014) Developing LBM process parameters for Ti-6Al-4V Thin Wall structures and determining the corresponding mechanical characteristics. *Phys Procedia* 56:90–98. <https://doi.org/10.1016/J.PHPRO.2014.08.102>
- Merklein M, Löffler M, Schneider T (2015) Plastic flow and its control in sheet-bulk metal forming of thin-walled functional components. *CIRP Ann - Manuf Technol*. <https://doi.org/10.1016/j.cirp.2015.04.078>
- Löffler M, Schulte R, Freiburg D et al (2019) Control of the material flow in sheet-bulk metal forming using modifications of the tool surface. *Int J Mater Form* 12:17–26. <https://doi.org/10.1007/s12289-018-1399-2>
- Schaub A, Ahuja B, Butzhammer L et al (2016) Additive manufacturing of functional elements on sheet metal. *Phys Procedia* 83:797–807. <https://doi.org/10.1016/j.phpro.2016.08.082>
- Papke T, Dubjella P, Butzhammer L et al (2018) Influence of a bending operation on the bonding strength for hybrid parts made of Ti-6Al-4V. *Procedia CIRP* 74:290–294. <https://doi.org/10.1016/j.procir.2018.08.113>
- Schaub A, Juechter V, Singer RF, Merklein M (2014) Characterization of hybrid components consisting of SEBM additive structures and sheet metal of alloy Ti-6Al-4V. *Key Eng Mater* 611–612:609–614. <https://doi.org/10.4028/www.scientific.net/KEM.611-612.609>
- Vairis Frost, M. A., Vairis A, Frost M (1998) High frequency linear friction welding of a titanium alloy. *Wear* 217:117–131 . doi: Doi [https://doi.org/10.1016/S0043-1648\(98\)00145-8](https://doi.org/10.1016/S0043-1648(98)00145-8)
- Vairis A, Frost M (1999) On the extrusion stage of linear friction welding of Ti 6Al 4V. *Mater Sci Eng A* 271:477–484. [https://doi.org/10.1016/S0921-5093\(99\)00449-9](https://doi.org/10.1016/S0921-5093(99)00449-9)
- Vairis A, Frost M (1998) High frequency linear friction welding of a titanium alloy. *Wear* 217:117–131 . doi: Doi [https://doi.org/10.1016/S0043-1648\(98\)00145-8](https://doi.org/10.1016/S0043-1648(98)00145-8)
- McAndrew AR, Colegrove PA, Bühr C et al (2018) A literature review of Ti-6Al-4V linear friction welding. *Prog Mater Sci* 92: 225–257
- Fratini Buffa, G., Cammalleri, M., Campanella, D. L (2013) On the linear friction welding process of aluminum alloys: experimental insights through process monitoring. *CIRP Ann - Manuf Technol* 62:295–298
- Kelly MR, Schmid SR, Adams DC et al (2019) Experimental investigation of linear friction welding of AISI 1020 steel with pre-heating. *J Manuf Process* 39:26–39. <https://doi.org/10.1016/j.jmapro.2019.01.038>
- Ma TJ, Tang LF, Li WY et al (2018) Linear friction welding of a solid-solution strengthened Ni-based superalloy: microstructure evolution and mechanical properties studies. *J Manuf Process* 34: 442–450. <https://doi.org/10.1016/j.jmapro.2018.06.011>
- Taban E, Gould JE, Lippold JC (2010) Dissimilar friction welding of 6061-T6 aluminum and AISI 1018 steel: properties and microstructural characterization. *Mater Des*. <https://doi.org/10.1016/j.matdes.2009.12.010>
- Wanjara P, Dalgaard E, Trigo G et al (2011) Linear friction welding of Al–Cu: part 1 – process evaluation. *Can Metall Q* 50:350–359. <https://doi.org/10.1179/000844311X13112418194644>
- Rao HM, Ghaffari B, Yuan W et al (2016) Effect of process parameters on microstructure and mechanical behaviors of friction stir linear welded aluminum to magnesium. *Mater Sci Eng A* 651:27–36. <https://doi.org/10.1016/j.msea.2015.10.082>
- Buffa G, Cammalleri M, Campanella D et al (2017) Linear friction welding of dissimilar AA6082 and AA2011 aluminum alloys: microstructural characterization and design guidelines. *Int J Mater Form* 10:307–315. <https://doi.org/10.1007/s12289-015-1279-y>
- Fratini L, Buffa G, Campanella D, La Spisa D (2012) Investigations on the linear friction welding process through numerical simulations and experiments. *Mater Des* 40:285–291. <https://doi.org/10.1016/j.matdes.2012.03.058>
- Buffa G, Campanella D, Pellegrino S, Fratini L (2016) Weld quality prediction in linear friction welding of AA6082-T6 through an integrated numerical tool. *J Mater Process Technol* 231:389–396. <https://doi.org/10.1016/j.jmatprotec.2016.01.012>
- Vairis Frost, M. A. (1999) On the extrusion stage of linear friction welding of Ti 6Al 4V. *Mater Sci Eng A* 271:477–484
- Baffari D, Buffa G, Campanella D et al (2019) Single block 3D numerical model for linear friction welding of titanium alloy. *Sci Technol Weld Join* 24:130–135. <https://doi.org/10.1080/13621718.2018.1492211>
- McAndrew AR, Colegrove PA, Addison AC et al (2015) Modelling the influence of the process inputs on the removal of surface contaminants from Ti-6Al-4V linear friction welds. *Mater Des* 66:183–195. <https://doi.org/10.1016/j.matdes.2014.10.058>

**Publisher's note** Springer Nature remains neutral with regard to jurisdictional claims in published maps and institutional affiliations.